JOURNAL OF Applied Polymer SCIENCE

Special Issue: Microfiltration and Ultrafiltration Membrane Science and Technology

Guest Editors: Prof. Isabel C. Escobar (University of Toledo) and Prof. Bart Van der Bruggen (University of Leuven)

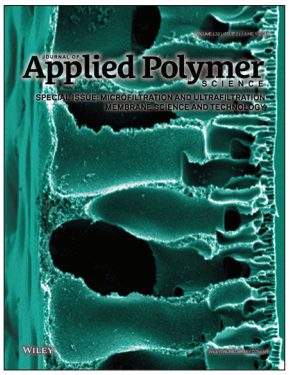

EDITORIAL

Microfiltration and Ultrafiltration Membrane Science and Technology
I. C. Escobar and B. Van der Bruggen, *J. Appl. Polym. Sci.* 2015, **DOI: 10.1002/app.42002**

REVIEWS

Nanoporous membranes generated from self-assembled block polymer precursors: *Quo Vadis*?
Y. Zhang, J. L. Sargent, B. W. Boudouris and W. A. Phillip, *J. Appl. Polym. Sci.* 2015, **DOI: 10.1002/app.41683**

Making polymeric membranes anti-fouling via "grafting from" polymerization of zwitterions
Q. Li, J. Imbrogno, G. Belfort and X.-L. Wang, *J. Appl. Polym. Sci.* 2015, **DOI: 10.1002/app.41781**

Fouling control on MF/ UF membranes: Effect of morphology, hydrophilicity and charge
R. Kumar and A. F. Ismail, *J. Appl. Polym. Sci.* 2015, **DOI: 10.1002/app.42042**

EMERGING MATERIALS AND FABRICATION

Preparation of a poly(phthalazine ether sulfone ketone) membrane with propanedioic acid as an additive and the prediction of its structure
P. Qin, A. Liu and C. Chen, *J. Appl. Polym. Sci.* 2015, **DOI: 10.1002/app.41621**

Preparation and characterization of MOF-PES ultrafiltration membranes
L. Zhai, G. Li, Y. Xu, M. Xiao, S. Wang and Y. Meng, *J. Appl. Polym. Sci.* 2015, **DOI: 10.1002/app.41663**

Tailoring of structures and permeation properties of asymmetric nanocomposite cellulose acetate/silver membranes
A. S. Figueiredo, M. G. Sánchez-Loredo, A. Maurício, M. F. C. Pereira, M. Minhalma and M. N. de Pinho, *J. Appl. Polym. Sci.* 2015, **DOI: 10.1002/app.41796**

LOW-FOULING POLYMERS

Low fouling polysulfone ultrafiltration membrane via click chemistry
Y. Xie, R. Tayouo and S. P. Nunes, *J. Appl. Polym. Sci.* 2015, **DOI: 10.1002/app.41549**

Elucidating membrane surface properties for preventing fouling of bioreactor membranes by surfactin
N. Behary, D. Lecouturier, A. Perwuelz and P. Dhulster, *J. Appl. Polym. Sci.* 2015, **DOI: 10.1002/app.41622**

PVC and PES-*g*-PEGMA blend membranes with improved ultrafiltration performance and fouling resistance
S. Jiang, J. Wang, J. Wu and Y. Chen, *J. Appl. Polym. Sci.* 2015, **DOI: 10.1002/app.41726**

Improved antifouling properties of TiO_2/PVDF nanocomposite membranes in UV coupled ultrafiltration
M. T. Moghadam, G. Lesage, T. Mohammadi, J.-P. Mericq, J. Mendret, M. Heran, C. Faur, S. Brosillon, M. Hemmati and F. Naeimpoor, *J. Appl. Polym. Sci.* 2015, **DOI: 10.1002/app.41731**

Development of functionalized doped carbon nanotube/polysulfone nanofiltration membranes for fouling control
P. Xie, Y. Li and J. Qiu, *J. Appl. Polym. Sci.* 2015, **DOI: 10.1002/app.41835**

JOURNAL OF Applied Polymer SCIENCE

Special Issue: Microfiltration and Ultrafiltration Membrane Science and Technology

Guest Editors: Prof. Isabel C. Escobar (University of Toledo) and
Prof. Bart Van der Bruggen (University of Leuven)

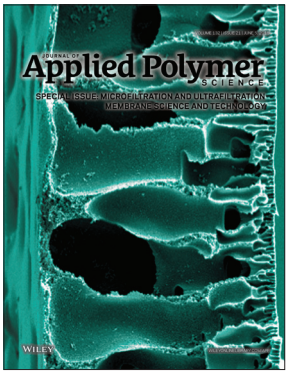

SURFACE MODIFICATION OF POLYMER MEMBRANES

Highly chlorine and oily fouling tolerant membrane surface modifications by *in situ* polymerization of dopamine and poly(ethylene glycol) diacrylate for water treatment
K. Yokwana, N. Gumbi, F. Adams, S. Mhlanga, E. Nxumalo and B. Mamba, *J. Appl. Polym. Sci.* 2015, **DOI: 10.1002/app.41661**

Fouling control through the hydrophilic surface modification of poly(vinylidene fluoride) membranes
H. Jang, D.-H. Song, I.-C. Kim, and Y.-N. Kwon, *J. Appl. Polym. Sci.* 2015, **DOI: 10.1002/app.41712**

Hydroxyl functionalized PVDF-TiO_2 ultrafiltration membrane and its antifouling properties
Y. H. Teow, A. A. Latif, J. K. Lim, H. P. Ngang, L. Y. Susan and B. S. Ooi, *J. Appl. Polym. Sci.* 2015, **DOI: 10.1002/app.41844**

Enhancing the antifouling properties of polysulfone ultrafiltration membranes by the grafting of poly(ethylene glycol) derivatives via surface amidation reactions
H. Yu, Y. Cao, G. Kang, Z. Liu, W. Kuang, J. Liu and M. Zhou, *J. Appl. Polym. Sci.* 2015, **DOI: 10.1002/app.41870**

SEPARATION APPLICATIONS

Experiment and simulation of the simultaneous removal of organic and inorganic contaminants by micellar enhanced ultrafiltration with mixed micelles
A. D. Vibhandik, S. Pawar and K. V. Marathe, *J. Appl. Polym. Sci.* 2015, **DOI: 10.1002/app.41435**

Polymeric membrane modification using SPEEK and bentonite for ultrafiltration of dairy wastewater
A. Pagidi, Y. Lukka Thuyavan, G. Arthanareeswaran, A. F. Ismail, J. Jaafar and D. Paul, *J. Appl. Polym. Sci.* 2015, **DOI: 10.1002/app.41651**

Forensic analysis of degraded polypropylene hollow fibers utilized in microfiltration
X. Lu, P. Shah, S. Maruf, S. Ortiz, T. Hoffard and J. Pellegrino, *J. Appl. Polym. Sci.* 2015, **DOI: 10.1002/app.41553**

A surface-renewal model for constant flux cross-flow microfiltration
S. Jiang and S. G. Chatterjee, *J. Appl. Polym. Sci.* 2015, **DOI: 10.1002/app.41778**

Ultrafiltration of aquatic humic substances through magnetically responsive polysulfone membranes
N. A. Azmi, Q. H. Ng and S. C. Low, *J. Appl. Polym. Sci.* 2015, **DOI: 10.1002/app.41874**

BIOSEPARATIONS APPLICATIONS

Analysis of the effects of electrostatic interactions on protein transport through zwitterionic ultrafiltration membranes using protein charge ladders
M. Hadidi and A. L. Zydney, *J. Appl. Polym. Sci.* 2015, **DOI: 10.1002/app.41540**

Modification of microfiltration membranes by hydrogel impregnation for pDNA purification
P. H. Castilho, T. R. Correia, M. T. Pessoa de Amorim, I. C. Escobar, J. A. Queiroz, I. J. Correia and A. M. Morão, *J. Appl. Polym. Sci.* 2015, **DOI: 10.1002/app.41610**

Hemodialysis membrane surface chemistry as a barrier to lipopolysaccharide transfer
B. Madsen, D. W. Britt, C.-H. Ho, M. Henrie, C. Ford, E. Stroup, B. Maltby, D. Olmstead and M. Andersen, *J. Appl. Polym. Sci.* 2015, **DOI: 10.1002/app.41550**

Membrane adsorbers comprising grafted glycopolymers for targeted lectin binding
H. C. S. Chenette and S. M. Husson, *J. Appl. Polym. Sci.* 2015, **DOI: 10.1002/app.41437**

Journal of Applied Polymer Science

Analysis of the effects of electrostatic interactions on protein transport through zwitterionic ultrafiltration membranes using protein charge ladders

Mahsa Hadidi, Andrew L. Zydney
Department of Chemical Engineering, The Pennsylvania State University, University Park, Pennsylvania, 16802
Correspondence to: A. Zydney (e-mail: zydney@engr.psu.edu)

ABSTRACT: A large number of studies have shown that zwitterionic ultrafiltration membranes have very low protein fouling due to the strongly hydrated structure of the zwitterionic modification. However, there is much less known about the effects of the zwitterionic functionality on the electrostatic interactions governing protein transport through these membranes. The objective of this work was to use protein charge ladders to evaluate the effects of electrostatic interactions on protein transport through cellulosic ultrafiltration membranes modified with a zwitterionic functionality. Data were obtained using protein charge ladders formed by reacting lysozyme and α-lactalbumin with acetic anhydride to generate a series of protein derivatives (ladders) differing by single charge groups but with essentially identical size. Protein retention was greater for the more positively charged elements within the charge ladder, consistent with a weak electrostatic repulsion from the zwitterionic membrane which had a small positive charge at pH 7. Data for all elements of the protein charge ladder (both positively and negatively charged) were in excellent agreement with calculations of a theoretical model based on the partitioning of a charged sphere (protein) in a charged cylinder. The results demonstrate the potential of using zwitterionic membranes for enhanced ultrafiltration with high selectivity and minimal fouling. © 2014 Wiley Periodicals, Inc. J. Appl. Polym. Sci. **2015**, *132*, 41540.

KEYWORDS: bioengineering; membranes; proteins

Received 23 July 2014; accepted 24 September 2014
DOI: 10.1002/app.41540

INTRODUCTION

Protein fouling remains one of the main factors limiting the application of ultrafiltration. Membrane modification is one of the many strategies used to reduce/control fouling effects since it reduces protein–membrane interactions.[1,2] Recent studies have shown that zwitterion-containing membranes strongly resist protein adsorption/fouling over a broad variety of ultrafiltration conditions.[3–5] This includes membranes made using a zwitterionic (sulfobetaine) copolymer[6,7] as well as membranes made by grafting zwitterionic ligands (e.g., sulfobetaine methacrylate) onto a base polymer membrane.[8] This low fouling behavior is typically attributed to the highly hydrated state of the zwitterionic functionality[9–12] which strongly excludes proteins from the membrane surface.[12,13]

However, there have been very few studies of the transport characteristics of these zwitterionic membranes. It is well known that protein transmission through narrow pore size membranes can be significantly reduced by electrostatic repulsive interactions between the proteins and the membrane.[14] This can not only provide opportunities for enhanced ultrafiltration with very high permeability membranes,[15] it can also be used to achieve highly selective protein separations based on differences in the net charge of the desired protein product and impurities.[16] Successful applications of this approach include the purification of monoclonal antibodies,[16] an antigen-binding fragment,[17] and pegylated proteins.[18]

Rohani and Zydney[19] performed one of the only studies of protein transmission through zwitterion-modified ultrafiltration membranes. Data were obtained with acidic, basic, and neutral proteins at different pH and ionic strength. The protein sieving coefficients were strongly correlated with the product of the effective protein and membrane charge densities. However, the use of several proteins with different net charge, surface charge distribution, and three-dimensional shape made it difficult to quantify the key phenomena governing the behavior of these zwitterionic membranes.

The objective of this study was to use protein charge ladders to develop a more fundamental and quantitative understanding of the electrostatic interactions governing protein transport through zwitterionic ultrafiltration membranes. Protein charge

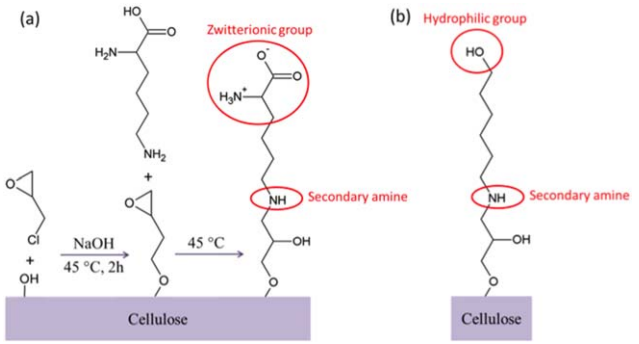

Figure 1. Schematic of the modification reactions used to prepare (a) the zwitterionic membrane and (b) the analogous hydrophilic membrane. [Color figure can be viewed in the online issue, which is available at wileyonlinelibrary.com.]

ladders were generated by chemical modification of lysozyme and α-lactalbumin with acetic anhydride, yielding a series of derivatives of the base protein differing by single charge groups. Data for the zwitterionic membrane were also compared with analogous results with a membrane containing a hydroxyl group in place of the zwitterion. Additional insights were obtained using available transport models based on the partition coefficient of a charged spherical protein in a charged cylindrical pore.

MATERIALS AND METHODS

Membranes

Zwitterionic ultrafiltration membranes were made by modification of Ultracel™ membranes (composite regenerated cellulose) with nominal molecular weight cut-off (MWCO) of 100 kDa (Millipore Corp., Massachusetts) using the chemistry described by Hadidi and Zydney.[20] Small membrane disks, cut from flat sheets, were soaked in isopropanol (90% by volume) for 45 min, and then thoroughly flushed with >100 L/m^2 of deionized (DI) water. Membranes were conditioned by soaking in 0.1 *M* NaOH for 24 hr and then activated by immersing in a mixture of one part epichlorohydrin (Alfa Aesar, A15823) and two parts 0.1 *M* NaOH (by volume) for 2 hr at 45°C. The membranes were then carefully removed and rinsed with DI water. Next, the epoxide rings on the pre-activated membranes were reacted by immersion in 20 mL of a 1 *M* solution of L-Lysine (Sigma, L5501) for 12 hr at 45°C as shown in Figure 1(a). Figure 1(b) shows the structure of an analogous hydrophilic membrane generated using 6-amino-1-hexanol (Sigma, A56353) instead of L-Lysine with the same coupling chemistry.

Membrane Characterization

The degree of surface modification was estimated by tracking the nitrogen peak in X-ray photoelectron spectroscopy (XPS). Small pieces of membrane (approximately 12 mm × 5 mm) were mounted on a sample platen for analysis. Data were obtained using a Kratos Analytical Axis Ultra instrument (Kratos Analytical Inc., New York) with monochromatic Al Kα X-ray source (1486.6 eV photons). Additional details are provided by Hadidi and Zydney.[20]

The effective charge of the zwitterion-modified membrane was determined from streaming potential measurements. The membrane was mounted between two Plexiglass chambers, with Ag/AgCl electrodes placed in the chambers (adjacent to both sides of the membrane) and connected to a multimeter. 10 m*M* buffered KCl solution at the desired pH was flowed through the membrane by air pressurization with the apparent zeta potential (ζ_{app}) calculated from the slope of the measured voltage (E_z) versus the transmembrane pressure (ΔP) using the Helmholtz-Smoluchowski equation:[21]

$$\zeta_{app} = \frac{\mu \Lambda_0}{\varepsilon_0 \varepsilon_r} \left(\frac{dE_z}{d\Delta P} \right), \quad (1)$$

where Λ_0 is the solution conductivity, the product of ε_0 and ε_r is the electrical permittivity of the solution, and μ is the solution viscosity.

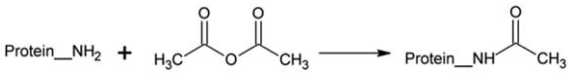

Figure 2. Graphic illustration of the acylation reaction using acetic anhydride.

Protein Charge Ladders

Protein charge ladders were generated by acylation of the lysine ε-amino groups of either lysozyme ($r_p = 2$ nm, 14.3 kDa, $pI = 11$) or α-lactalbumin ($r_p = 2$ nm, 14.2 kDa, $pI = 4.6$) using acetic anhydride (Sigma 242845) following the procedure described by Chung *et al.*[22] (Figure 2). The acylation reaction converts the protonatable amino group into a neutral amide, thereby reducing the number of positive charge groups on the protein. Charge ladders were prepared using 10 g/L solutions of the desired protein. The pH was set to 12 using 1 *N* NaOH. Approximately four equivalents (per mole of protein) of 0.1 *M* acetic anhydride in 1,4-dioxane (Sigma 360481) were added to the protein solution, with the reaction quenched after 5 min using 1 *M* HCl. The resulting solution was diafiltered through an Ultracel 10 kDa membrane at low pressure (approximately 7 kPa) using about four diavolumes of chilled DI water to remove the dioxane, unreacted acetic anhydride, and any reaction by-products. Another diafiltration process was performed using at least four diavolumes of chilled buffer to put the protein in the desired buffer solution. Protein solutions were stored at 2°C–8°C to reduce the extent of protein aggregation or denaturation.

The concentration of each element of the charge ladder was evaluated using a High-Performance Capillary Electrophoresis instrument (Agilent Technologies, California). The G1600A instrument was equipped with a dual polarity variable high voltage DC power supply and variable wavelength UV-vis diode array detector. Negatively charged fused silica capillaries (Agilent Technologies, G 1600–61211, California) were used for the negatively charged α-lactalbumin, and positively charged eCAP™ Amine capillaries (Beckman Coulter, Inc., 477431, Fullerton, CA) were used for the positively charged lysozyme to minimize protein adsorption to the capillary wall. Both capillaries had 50 μm inner diameter and were 65 cm in length (effective length of approximately 55 cm). Protein concentrations were determined by the absorbance at 214 nm. Mesityl oxide (Fluka 63940) was used as a neutral marker. Both capillaries were

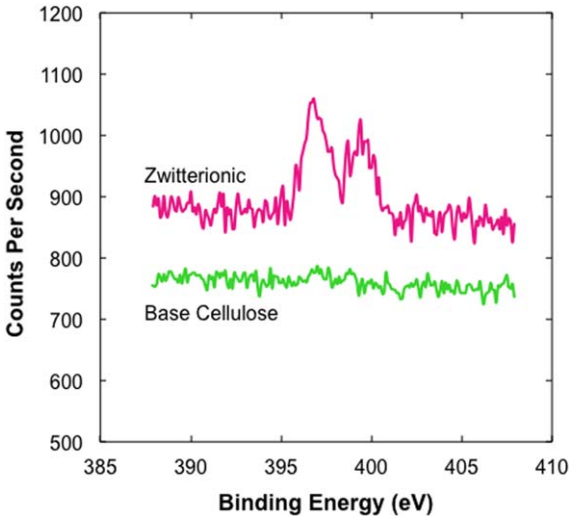

Figure 3. Nitrogen peak in the XPS spectra for the zwitterionic membrane and the base Ultracel 100 kDa membrane. Adapted from Hadidi and Zydney.[20] [Color figure can be viewed in the online issue, which is available at wileyonlinelibrary.com.]

flushed with 0.1 *M* NaOH for 10 min followed by the running buffer [10 m*M* KCl with 192 m*M* glycine (Sigma G7403) and 25 m*M* Trizma® base (Sigma T1503) at pH 8.3] for an additional 10 min. Additionally, an amine regenerator solution (Beckman Coulter, Inc., 477433) was used to regenerate the eCAP™ Amine capillary between runs. 15–30 nL samples were injected by application of a 3.5 kPa pressure for 25 s. Electrophoresis was carried out at an applied voltage of 25 kV with the direction of the electric field set so that the electroosmotic flow was toward the outlet of the capillary. The current was kept below 45 μA to minimize Joule heating. ChemStation software (3D-CE, Version A.0903, Agilent Technologies, California) was used to record and analyze the electropherograms. Additional experimental details are available elsewhere.[23,24]

Ultrafiltration

Ultrafiltration experiments were conducted in a stirred Amicon cell (Model 8010, Millipore Corp.). A porous Tyvek® support was placed under the membrane in the bottom of the cell for support. The cell was filled with a solution of 10 m*M* KCl buffered with 1 m*M* BisTris (MPBiomedicals 101038) at pH 7. The hydraulic permeability (L_p) of the membrane was calculated from the slope of data for the filtrate flux (measured by timed collection) as a function of the transmembrane pressure as:

$$L_p = \frac{\mu J_v}{\Delta P}, \tag{2}$$

where μ is the solution viscosity, J_v is the filtrate flux, and ΔP is the transmembrane pressure.

The stirred cell was then emptied, filled with the protein charge ladder solution, and connected to a feed reservoir containing the charge ladder solution. The stirred cell was placed on a magnetic stir plate with the stirring speed set to 600 rpm using a Strobotac (General Radio Co.). The system was air-pressurized to approximately 10 kPa (1.5 psi), with filtrate samples collected after filtration of at least 500 μL to reach equilibrium operation and clear the dead volume under the membrane. The observed sieving coefficient for each element of the charge ladder was calculated as:

$$S_o = \frac{C_f}{C_b}, \tag{3}$$

where C_f and C_b are the concentrations of each specific element in the filtrate and bulk solutions, respectively, as determined from the capillary electropherogram.

RESULTS AND DISCUSSIONS

Membrane Modification

The effectiveness of the membrane surface modification was evaluated by X-ray photoelectron spectroscopy (XPS) by focusing on the peak associated with the nitrogen binding energy (398 eV), which is completely absent in the base cellulose. The double peak seen with the zwitterionic membrane (Figure 3) arises from the two distinct nitrogens: a primary amine in the zwitterionic functionality and a secondary amine formed by the reaction that couples the lysine to the base cellulose (see schematic in Figure 1).

The degree of modification was calculated based on the atomic composition of the zwitterionic membrane determined from the peak areas associated with the C, O, and N atoms in the XPS spectra (Table I). The best fit value of the degree of modification (f), defined as the fraction of glucose rings in the base cellulose membrane that were linked to the zwitterion, was determined by comparison of the calculated atomic fraction of each element with the experimental data. For example, the nitrogen fraction (F_N) was calculated as:

$$F_N = \frac{af}{b + af} \tag{4}$$

where a, b, and d are determined from the atomic structure of the zwitterionic membrane: $a = 2$ (accounting for the two nitrogens in the lysine ligand), $b = 11$ (from the 6 carbon and 5 oxygen atoms in a single glucose ring of the cellulose), and $d = 14$ (from the 3 C and 1 O in the epichlorohydrin activation and the 6 C, 2 N, and 2 O in the structure of the zwitterionic ligand). Similar equations were used for carbon and oxygen. The best fit value of $f = 0.025 \pm 0.004$ was determined by minimizing the sum of the squares of the normalized residuals, with the results in excellent agreement with the composition determined from the peak areas (Table I).

Membrane Surface Charge

The surface charge characteristics of the zwitterion-modified membrane were determined from streaming potential measurements as shown in Figure 4. Data were obtained using 10 m*M* KCl solutions at different pH. The streaming potential increased with increasing pressure at pH 6, 7, and 8, corresponding to an effective positive charge on the membrane. This positive charge is due primarily to the secondary amine involved in the linkage of the zwitterion to the cellulose membrane. The slope, and thus the effective charge, was negative at pH 9 and 10 where both of the amine groups become un-protonated.

The apparent zeta potential was calculated directly from the data in Figure 4 using the Helmholtz-Smoluchowski equation

Table I. Comparison of the Measured (Peak Area in XPS) and Calculated Atomic Composition (in Percent) of the Zwitterionic Membrane

	N content	C content	O content
Peak area-XPS	0.44	54.8	44.7
Best fit	0.44	54.8	44.7

(eq. (1)), with the results summarized in Figure 5. The data are plotted as a function of the partial zwitterion charge calculated from the pK_a values for the ionizable groups in the zwitterionic ligand: 9.06 for the primary amine, 2.16 for the carboxylic acid, and 8.8 for the secondary amine in the linkage to the base cellulose (estimated).[25] The small difference between the pK_a values of the two amine groups reflects the shift in electron density within the ligand. The value for the secondary amine was estimated as 8.8, which is well below the pK_a of the second amine group in lysine (10.54), based on the reported differences in pK_a for taurine (9.08) and N-[Tris(hydroxymethyl)methyl]-2-aminoethanesulfonic acid or TES (7.34), two analogs in which the primary amine in taurine has been replaced with a secondary amine in TES.[19] The partial charge of each group was calculated using the Henderson-Hasselbach equation:

$$\mathrm{pH} = pK^{i}_{\mathrm{int}} + log\frac{r_i}{(n_i - r_i)}, \quad (5)$$

where n_i is the total number of titratable species and r_i is the number of dissociated groups. The results are linear when plotted in this fashion, with $r^2 = 0.98$, indicating that the effective charge of the zwitterionic membrane is determined directly by the protonation/deprotonation of the ionizable functionalities within the zwitterionic ligand. However, the isoelectric point of the membrane (where $\zeta_{app} = 0$) occurs at a point where the calculated fractional charge is slightly positive. This could be due to an error in the estimated value of pK_a for the secondary amine; calculations performed using a pK_a value of 8.2 shifts the fit so that the isoelectric point of the membrane occurs at a calculated fractional charge of zero.

Charge Ladder Ultrafiltration

Figure 6 shows typical capillary electropherograms for 5 g/L solutions of the α-lactalbumin [Figure 6(a)] and lysozyme [Figure 6(b)] charge ladders in a 10 m*M* ionic strength Tris/glycine buffer at pH 8.3. The charged species migrate back against the electroosmotic flow due to electrophoresis so that they pass the detector after the neutral marker. Thus, the first peak in the electropherogram for α-lactalbumin represents the neutral marker followed by the unmodified lactalbumin (which has the smallest negative charge) and then the other protein derivatives, each of which has one less positive amine group (i.e., one more negative charge). Thirteen peaks (rungs) are seen in the electropherogram, corresponding to 0–12 acylated lysine groups. The electropherogram for the lysozyme charge ladder begins with the neutral marker followed by the most highly modified lysozyme species (with lowest net positive charge at this pH), with the unmodified lysozyme eluting as the last peak. It is just possible to make out seven rungs in the charge ladder, consistent with the six lysine residues in lysozyme.

Figure 7 shows typical data for the ultrafiltration of the lysozyme charge ladder through the zwitterionic membrane at pH 7 using a 10 m*M* ionic strength solution. The data were obtained at a transmembrane pressure of 10 kPa (1.5 psi) and 600 rpm stirring speed, giving a filtrate flux of 4 μm/s. There was no evidence of any fouling during this experiment, with the permeability measured after the ultrafiltration ($L_p = 3.3\times10^{-12}$m) being within 10% of that measured immediately before the filtration experiment. This behavior is consistent with the low-fouling of the zwitterionic membrane reported previously by Hadidi and Zydney[20] using unmodified lysozyme (not a lysozyme charge ladder) as well as with α-lactalbumin, bovine serum albumin, and IgG. Results are shown for the seven

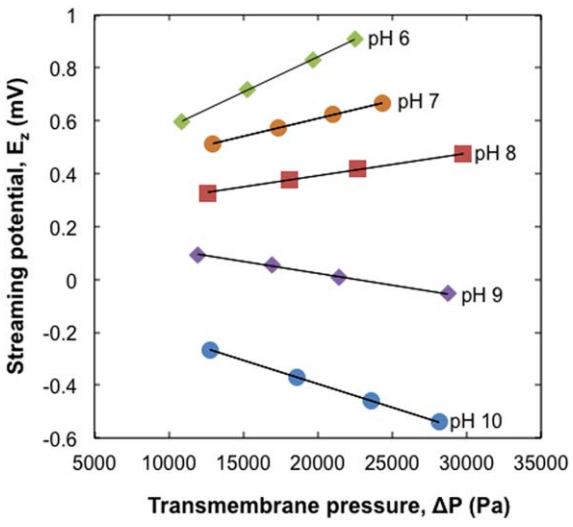

Figure 4. Streaming potential data as a function of transmembrane pressure for the zwitterionic membrane over a range of pH. Taken from Hadidi and Zydney.[20] [Color figure can be viewed in the online issue, which is available at wileyonlinelibrary.com.]

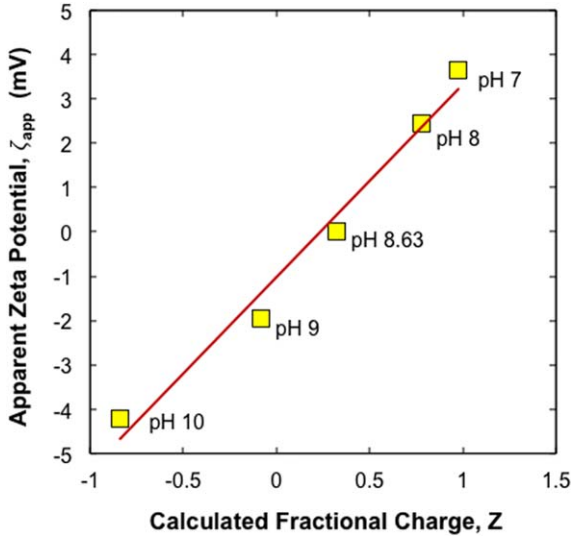

Figure 5. Experimental data for the apparent zeta potential as a function of the fractional charge calculated based on the pK_a values of the zwitterionic ligand. [Color figure can be viewed in the online issue, which is available at wileyonlinelibrary.com.]

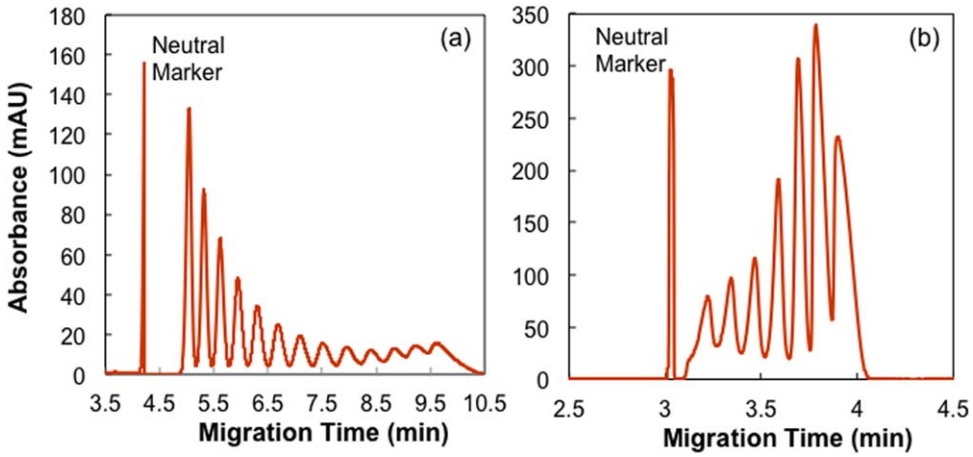

Figure 6. Capillary electropherograms for charge ladders made from (a) α-lactalbumin and (b) lysozyme in 10 m*M* Tris/glycine buffer at pH 8.3. [Color figure can be viewed in the online issue, which is available at wileyonlinelibrary.com.]

elements or "rungs" of the lysozyme charge ladder (i.e., the individual peaks in the capillary electropherogram). In each case, the observed sieving coefficient was calculated as the ratio of the protein concentration in the filtrate solution to that in the feed, with the concentration of each rung (peak) of the charge ladder evaluated directly from the capillary electropherogram by numerical integration of the peak area (defined by the local minima in the electropherogram). The data are plotted as a function of the peak number in the charge ladder, with seven corresponding to the native lysozyme and six corresponding to the first peak to the left of lysozyme (corresponding to the lysozyme with one acylated amino group). Thus, the results in Figure 7 represent data obtained in a single ultrafiltration experiment, without any complications from lot-to-lot variations in membrane properties and/or small differences in membrane fouling. The sieving coefficients decrease with increasing peak number, consistent with the small positive charge on the zwitterionic membrane at pH 7 and the reduction in the net positive charge of the elements in the lysozyme charge ladder with increasing numbers of acylated lysine groups. Note that the native lysozyme has a net charge of approximately 7.2 at pH 7 reflecting the high isoelectric point of this protein ($pI = 11$).

The filled diamonds in Figure 7 represent data from a corresponding experiment performed with an Ultracel 100 kDa membrane modified using the same chemistry as that used to generate the zwitterionic membrane but with 6-amino-1-hexanol used in place of lysine.[20] This ligand is nearly the same size as lysine, but the zwitterionic group at the end of the lysine is replaced with a hydroxyl group [see Figure 1(a,b)]; both ligands are attached to the base cellulose via a secondary amine. The zeta potential for this "hydrophilic" membrane at pH 7 was +3.0 mV, which is identical to that measured with the zwitterionic membrane, consistent with the charge on both membranes arising from the secondary amine. As seen in Figure 7, the observed sieving coefficients for the hydrophilic membrane are almost identical to those for the zwitterionic membrane for all seven peaks in the lysozyme charge ladder, suggesting that the zwitterionic functionality behaves much as an uncharged hydroxyl group, at least in terms of its effect on protein transmission through a narrow pore. This is discussed in more detail subsequently.

Theoretical Analysis

In order to obtain a more detailed understanding of the ultrafiltration behavior, the observed sieving coefficient data were analyzed using a well-established model that accounts for the effects of electrostatic interactions on protein transport in narrow pores.[26] The actual sieving coefficient of the protein, $S_a = C_f/C_w$ where C_w is the protein concentration at the membrane surface, is expressed as:

$$S_a = \varnothing \; K_c, \tag{6}$$

where $\varnothing$ is the partition coefficient of the protein between the bulk solution and the membrane pore and K_c is the convection hindrance factor, accounting for the hydrodynamic drag on the protein from the pore wall. Equation (6) assumes convection dominant

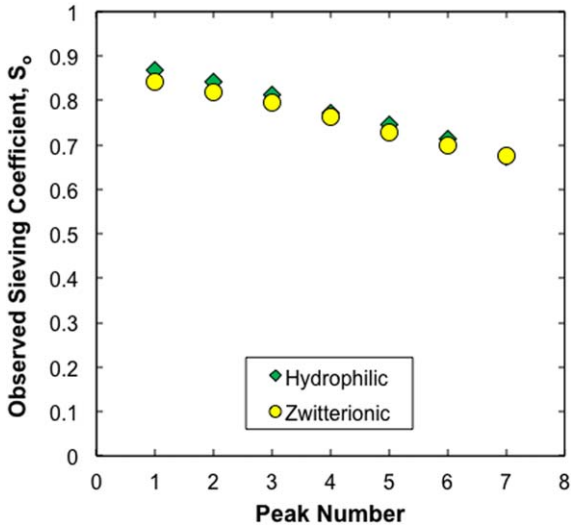

Figure 7. Observed sieving coefficients for ultrafiltration of the lysozyme charge ladder through the zwitterionic membrane at pH 7, 10 m*M* ionic strength, and 10 kPa. Diamonds represent data obtained with an analogous hydrophilic membrane. [Color figure can be viewed in the online issue, which is available at wileyonlinelibrary.com.]

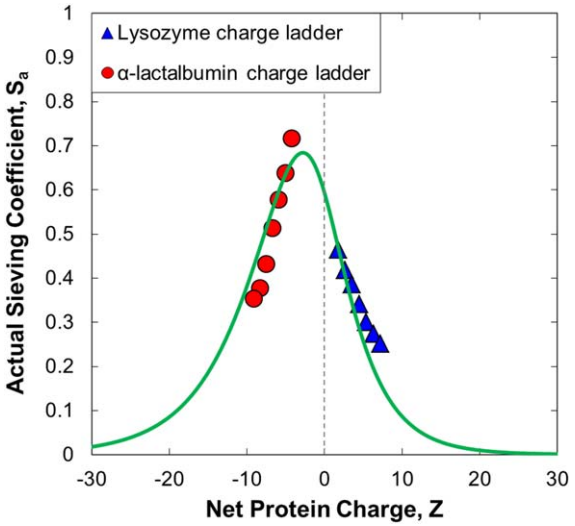

Figure 8. Actual sieving coefficients for elements in the lysozyme and α-lactalbumin charge ladders through the zwitterionic membrane at pH 7 and 10 m*M* ionic strength. Data are plotted as a function of the net protein charge calculated from the amino acid composition. Solid curve is the model prediction as described in the text. [Color figure can be viewed in the online issue, which is available at wileyonlinelibrary.com.]

protein transport, which is an appropriate assumption, based on the Peclet numbers in protein ultrafiltration systems.

The equilibrium partition coefficient is evaluated as the average protein concentration inside the membrane pore divided by that in the bulk (or filtrate) solution adjacent to the pore:

$$\varnothing = \frac{C_{z=0}}{C_w} = \frac{C_{z=\delta}}{C_f} = \exp\left[-\frac{\Psi_{\text{total}}}{k_B T}\right], \tag{7}$$

where T is the absolute temperate, k_B is the Boltzmann constant, and Ψ_{total} is the total interaction potential. The interaction potential for a uniformly charged sphere in a uniformly charged cylinder at constant surface charge density can be expressed as:[26]

$$\frac{\Psi_E}{k_B T} = (A_s \sigma_s^2 + A_{sp}\sigma_s\sigma_p + A_p\sigma_p^2)/A_{den} \tag{8}$$

where the coefficients A_s, A_{sp}, A_p, and A_{den} are all positive functions of the solution ionic strength and the solute and pore radii. σ_p and σ_s are the dimensionless surface charge densities of the pore and solute. Expressions for all the key parameters are provided elsewhere.[14,27]

The net electrical charge of each element in the protein charge ladder was evaluated from its amino acid sequence accounting for the acylation of one or more lysine amino groups. The number of dissociated amino acid residues was calculated from the intrinsic dissociation constant for each amino acid (see Appendix) using the Henderson-Hasselbach equation (eq. (5)) with the local H^+ concentration related to the bulk concentration using a classical Boltzmann distribution:

$$H^+ = H_b^+ \exp\left(\frac{-e\Psi_s}{k_B T}\right), \tag{9}$$

where H_b^+ is the hydrogen ion concentration in the bulk solution, e is the charge of the electron, and Ψ_s is the electrostatic potential at the protein surface:

$$\Psi_s = \frac{eZ}{4\pi\varepsilon_0\varepsilon_r r_s(1+\kappa r_s)}, \tag{10}$$

where Z is the net protein surface charge. Equation (10) is valid for a hard sphere uniformly charged over the surface.[28] The net protein charge is evaluated as the difference between the maximum number of positive charges and the sum of all the dissociated groups:

$$Z = Z_{\max}^+ - \sum_{i=1}^{n} r_i. \tag{11}$$

The observed sieving coefficient data from Figure 7, along with corresponding data obtained with the α-lactalbumin charge ladder, have been plotted in Figure 8 in terms of the actual protein sieving coefficient as a function of the net protein charge. The actual sieving coefficient was calculated from the S_o data using a simple stagnant film model accounting for concentration polarization effects:[29]

$$S_a = \frac{S_o}{(1-S_o)\exp\left(\frac{J_v}{k}\right) + S_o}, \tag{12}$$

where J_v is the filtrate flux and $k_m = 2.1 \times 10^{-6}$ m/s is the mass transfer coefficient in the stirred ultrafiltration cell calculated using available correlations. Equation (12) ignores the effects of electrostatic interactions on boundary layer transport, which should be a reasonable approximation given that the concentration boundary layer in the stirred cell (on the order of 100 μm) is much larger than the thickness of the electrical double layer (approximately 3 nm in a 10 m*M* ionic strength solution). The elements in the α-lactalbumin charge ladder are all negatively charged at pH 7, with the peak at $Z = -4.2$ corresponding to the unmodified protein. There was some evidence of a small amount of fouling in the run with the α-lactalbumin charge ladder, most likely due to the attractive electrostatic interactions between the negatively charged proteins and the positively charged membrane. This behavior is similar to that reported by Chang *et al.*[30] for pseudo-zwitterionic membranes made from mixed positive and negative charge functionalities under conditions where there was a small net charge due to an imbalance between the positive and negative ligands. However, it is important to note that the measured transmission of the α-lactalbumin remained above 75% for all elements of the charge ladder.

The solid curve in Figure 8 represents the predicted values of the actual sieving coefficient. The membrane was assumed to have a log-normal pore size distribution[30] with the mean pore radius determined from measurements of dextran retention as described in the Appendix. Thus, all of the model parameters were evaluated independently: the charge of the elements of the protein ladder were determined from the amino acid sequence, the membrane charge was determined from the streaming potential, and the membrane pore size was determined from the dextran data. The actual sieving coefficients for each element of the charge ladder were then evaluated by integrating eqs. (6) and (7) over the pore size distribution, with the hindrance factor evaluated using available hydrodynamic models in terms of the ratio of the solute to pore radius.[31]

The model predictions are in excellent agreement with the experimental data for both charge ladders, although the model does overestimate the results for the more heavily charged species in the lysozyme charge ladder. The maximum theoretical value of the sieving coefficient occurs at $Z = -2.8$, with the attractive contribution to the electrostatic energy of interaction (the term involving the product of the surface charge densities of the protein and pore in eq. (8)), giving rise to an increase in the sieving coefficient compared to that for an uncharged protein. The sieving coefficient decreases as the protein becomes more negatively charged due to the energetic penalty arising from the distortion of the electrical double layer around the protein as described by the term involving the square of the protein surface charge density in the energy of interaction (eq. (8)). The net result is that the sieving coefficient for the most negatively charged species in the α-lactalbumin charge ladder ($S_a = 0.34$) is well below that for first element in the lysozyme charge ladder ($S_a = 0.45$), even though the lysozyme has the same polarity as the membrane while the α-lactalbumin is oppositely charged. The agreement between the theoretical model and the experimental data demonstrates that the effects of electrostatic interactions on protein transport through the zwitterionic membrane are similar to those for charged membranes (with the membrane surface charge in both cases determined directly from the apparent zeta potential).

CONCLUSIONS

Although previous studies have clearly shown the low fouling properties of zwitterionic membranes, much less is known about the transport characteristics of these novel porous materials. In this work, we used protein charge ladders, consisting of a series of protein variants with the same physical size/structure but with different surface charge, to evaluate the effects of electrostatic interactions on the sieving characteristics of a zwitterionic membrane made by the attachment of a lysine amino acid to a commercially available cellulose membrane. The use of protein charge ladders eliminates complications associated with differences in membrane charge (for experiments done at different pH), protein structure (for experiments with different proteins), and lot-to-lot variability while allowing data to be obtained over a range of protein charge in a single experiment.

The transmission of the elements within the protein charge ladder through the zwitterionic membrane was nearly identical to that for a corresponding membrane made using the same chemistry but with a hydroxyl group replacing the zwitterionic functionality. Thus, the zwitterionic group appears to behave analogous to an uncharged hydrophilic (hydroxyl) group in the context of protein transport, with the electrostatic interactions dominated by the small positive charge associated with the secondary amine used to link the zwitterion to the base cellulose. The experimental data for both the lysozyme and α-lactalbumin charge ladders were in excellent agreement with model predictions based on a uniformly charged sphere and cylinder, with all of the key physical parameters evaluated from independent experimental measurements (e.g., the membrane pore size and charge) or computations (e.g., the charge of the individual elements within the charge ladder). The results with the α-lactalbumin show the effects of attractive electrostatic charge-charge interactions, which dominate for the weakly charged elements in the charge ladder, as well as the repulsive interactions that arise from the energetic penalty associated with the distortion of the electrical double layer around the protein (for the more heavily charged elements). The dominance of the double layer repulsion, even for solutes that are oppositely charged to the membrane, has rarely been seen in previous experimental studies due to the fouling that typically occurs under these conditions. The different effects of the zwitterionic functionality on protein transport and fouling is likely due to the different length scales involved in these processes. Protein transmission through the charged pores is dominated by longer range electrostatic interactions (over a length scale of the double layer thickness, which is approximately 3 nm in the 10 m*M* ionic strength solutions), while fouling is due to much shorter range interactions between the protein and membrane surface (over a length scale of only a few angstroms).

These results suggest that these zwitterionic membranes may be able to provide the enhanced permeability and selectivity that have been demonstrated previously with electrically charged membranes while maintaining very low fouling characteristics due to the presence of the zwitterionic functionality at the outer portion of the ligand. Additional experimental studies will be needed to confirm this hypothesis and to provide further demonstration of the potential of these zwitterionic membranes for high performance protein ultrafiltration.

APPENDIX

The number and pK_a values of the various amino acids present in lysozyme and α-lactalbumin used in this work are presented in Tables AI and AII. Calculations for the charge ladders were performed by eliminating one lysine amino acid residue for

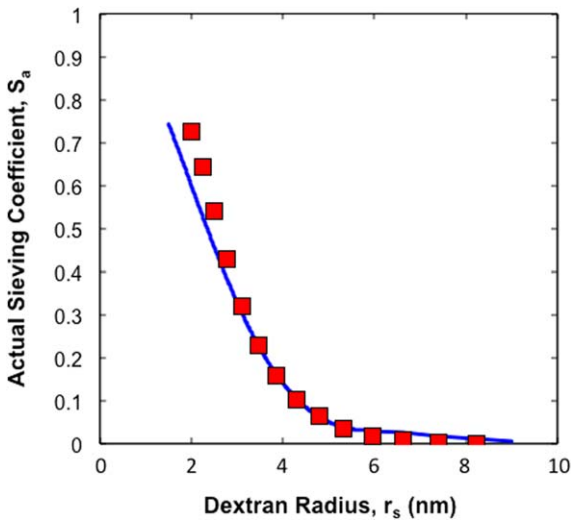

Figure A1. Comparison of model calculations and experimental data for the actual dextran sieving coefficients through the zwitterionic membrane in a 150 m*M* ionic strength solution at pH 7 and a flux of 4 μm/s. [Color figure can be viewed in the online issue, which is available at wileyonlinelibrary.com.]

Table AI. Number and pK^i_{int} Values of Ionizable Amino Acids in Lysozyme

Type	n_i	pK^i_{int}
α-Amino	1	7.5
His	1	6.3
Arg	11	12.5
Lys	6	10.5
Glu	2	4.4
Asp	7	4
α-carboxyl	1	3.8
Tyr	3	9.6

each element of the ladder (due to reaction with acetic anhydride).

Experimental data for the actual dextran sieving coefficients through the zwitterionic membrane as a function of the dextran radius are shown in Figure A1. The ultrafiltration was performed using a polydisperse dextran solution in a 150 m*M* ionic strength buffer at pH 7 and a pressure of 10 kPa giving a filtrate flux of 4 μm/s. The observed sieving coefficients were evaluated using size exclusion chromatography, with the concentrations in the filtrate and bulk solutions determined using a refractive index detector. The actual sieving coefficients were then calculated from the S_o data using eq. (12). The dextran radius was determined from available correlations, with the molecular weight based on results for dextran standards.[31] The solid curve is developed using eq. (6) with the partition coefficient and the hindrance factor evaluated using available hydrodynamic models assuming that the membrane has a log-normal pore size distribution with coefficient of variation (ratio of standard deviation to the mean) equal to 0.2.[31] The results give a best fit pore size of 4.9 nm, with the model calculations in good agreement with the data over the full range of dextran size.

ACKNOWLEDGMENTS

The authors would like to thank Millipore Corporation for donation of the Ultracel™ membranes and the Material Research Institute at The Pennsylvania State University for assistance with the XPS measurements.

Table AII. Number and pK^i_{int} Values of Ionizable Amino Acids in α-Lactalbumin

Type	n_i	pK^i_{int}
N-term	1	9.87
His	3	6.04
Arg	0	12.5
Lys	12	10.54
Glu	8	3.9
Asp	9	3.9
C-term	1	2.16
Tyr	4	10.3

REFERENCES

1. Pasmore, M.; Todd, P.; Smith, S.; Baker, D.; Silverstein, J.; Coons, D.; Bowman, C. N. *J. Membr. Sci.* **2001**, *194*, 15.
2. Vrijenhoek, E. M.; Hong, S.; Elimelech, M. *J. Membr. Sci.* **2001**, *188*, 115.
3. Li, Q.; Bi, Q.-Y.; Liu, T.-Y.; Wang, X.-L. *Appl. Surf. Sci.* **2012**, *258*, 7480.
4. Chiang, Y.-C.; Chang, Y.; Higuchi, A.; Chen, W.-Y.; Ruaan, R.-C. *J. Membr. Sci.* **2009**, *339*, 151.
5. Zhao, Y.-H.; Wee, K.-H.; Bai, R. *J. Membr. Sci.* **2010**, *362*, 326.
6. Sun, Q.; Su, Y.; Ma, X.; Wang, Y.; Jiang, Z. *J. Membr. Sci.* **2006**, *285*, 299.
7. Wang, T.; Wang, Y.-Q.; Su, Y.-L.; Jiang, Z.-Y. *J. Membr. Sci.* **2006**, *280*, 343.
8. Razi, F.; Sawada, I.; Ohmukai, Y.; Maruyama, T.; Matsuyama, H. *J. Membr. Sci.* **2012**, *401*, 292.
9. Li, M.-Z.; Li, J.-H.; Shao, X.-S.; Miao, J.; Wang, J.-B.; Zhang, Q.-Q.; Xu, X.-P. *J. Membr. Sci.* **2012**, *405*, 141.
10. Nagumo, R.; Akamatsu, K.; Miura, R.; Suzuki, A.; Tsuboi, H.; Hatakeyama, N.; Takaba, H.; Miyamoto, A. *Ind. Eng. Chem. Res.* **2012**, *51*, 4458.
11. Chen, S.; Zheng, J.; Li, L.; Jiang, S. *J. Am. Chem. Soc.* **2005**, *127*, 14473.
12. Ishihara, K.; Nomura, H.; Mihara, T.; Kurita, K.; Iwasaki, Y.; Nakabayashi, N. *J. Biomed. Mater. Res.* **1998**, *39*, 323.
13. Liu, J.; Zhan, Y.; Xu, T.; Shao, G. *J. Membr. Sci.* **2008**, *325*, 495.
14. Rohani, M. M.; Zydney, A. L. *Adv. Colloid Interface Sci.* **2010**, *160*, 40.
15. Mehta, A.; Zydney, A. L. *J. Membr. Sci.* **2005**, *249*, 245.
16. van Reis, R.; Zydney, A. *J. Membr. Sci.* **2007** *297*, 16.
17. Van Reis, R.; Brake, J.; Charkoudian, J.; Burns, D.; Zydney, A. L. *J. Membr. Sci.* **1999**, *159*, 133.
18. Ruanjaikaen, K.; Zydney, A. L. *Biotechnol. Bioeng.* **2011**, *108*, 822.
19. Rohani, M. M.; Zydney, A. L. *J. Membr. Sci.* **2012**, *397*, 1.
20. Hadidi, M.; Zydney, A. L. *J. Membr. Sci.* **2014**, *452*, 97.
21. Hunter, R. J. Zeta Potential in Colloid Science: Principles and Applications; Academic Press: London, **1981**.
22. Chung, W. K.; Evans, S. T.; Freed, A. S.; Keba, J. J.; Baer, Z. C.; Rege, K.; Cramer, S. M. *Langmuir* **2009**, *26*, 759.
23. Menon, M. K.; Zydney, A. L. *J. Membr. Sci.* **2001**, *181*, 179.
24. Gao, J.; Gomez, F. A.; Härter, R.; Whitesides, G. M. *Proc. Natl. Acad. Sci. USA* **1994**, *91*, 12027.
25. Brown, T. A. Molecular Biology Labfax: Recombinant DNA; Academic Press: San Diego, **1998**.
26. Smith, F. G.; Deen, W. M. *J. Colloid Interface Sci.* **1980**, *78*, 444.
27. Burns, D. B.; Zydney, A. L. *AIChE J.* **2001**, *47*, 1101.
28. Overbeek, J. T. G.; Wiersema, P. H. *Electrophoresis* **1967**, *2*, 1.
29. Zydney, A. L. *J. Membr. Sci.* **1997**, *130*, 275.
30. Chang, Y.; Shu, S.-H.; Shih, Y.-J.; Chu, C.-W.; Ruaan, R.-C.; Chen, W.-Y. *Langmuir* **2010**, *26*, 3522.
31. Zeman, L. J.; Zydney, A. L. Microfiltration and Ultrafiltration: Principles and Applications; Marcel Dekker: New York, **1996**.